

# Spatial pattern formation induced by Gaussian white noise

Stefania Scarsoglio<sup>a</sup>, Francesco Laio<sup>a</sup>, Paolo D’Odorico<sup>b</sup>, Luca Ridolfi<sup>a</sup>

<sup>a</sup>*Dipartimento di Idraulica, Trasporti ed Infrastrutture Civili, Politecnico di Torino, Torino, Italy*

<sup>b</sup>*Department of Environmental Sciences, University of Virginia, Charlottesville, Virginia, USA*

---

## Abstract

The ability of Gaussian noise to induce ordered states in dynamical systems is here presented in an overview of the main stochastic mechanisms able to generate spatial patterns. These mechanisms involve: (i) a deterministic local dynamics term, accounting for the local rate of variation of the field variable, (ii) a noise component (additive or multiplicative) accounting for the unavoidable environmental disturbances, and (iii) a linear spatial coupling component, which provides spatial coherence and takes into account diffusion mechanisms. We investigate these dynamics using analytical tools, such as mean-field theory, linear stability analysis and structure function analysis, and use numerical simulations to confirm these analytical results.

**Keywords:** spatial patterns, noise-induced phenomena, Gaussian white noise

---

## 1. Introduction

Spatial patterns are widely present in different natural dynamical systems. Their occurrence has been studied for quite a long time with applications to different fields, including for example hydrodynamic systems (e.g. Rayleigh-Bénard convection [1, 2]) and biochemical and neural systems (see, for instance, [3, 4]). In particular, a number of environmental processes are known for their ability to develop highly organized spatial features. For example, remarkable degrees of coherence can be found in the spatial distribution of dryland and riparian vegetation [5, 6, 7, 8]), river channels [9, 10, 11], coastlines [12, 13], sand ripples and dunes [14]. Figure 1 shows an example of natural spatial patterns around the world. These patterns exhibit amazing regular configurations. Found over areas of up to several square kilometers, they can occur on different soils and with a broad variety of vegetation species and life forms [15, 16, 17, 18].

The study of patterns can offer useful information on the underlying processes causing possible changes in the system. In recent years, several authors have investigated the mechanisms of pattern formation in nature, and their response to changes in environmental conditions or disturbance regime. For example, in the case of landscape ecology, these studies have related vegetation patterns to the underlying eco-hydrological processes [7, 19, 20], the nature of the interactions among plant individuals [6, 19], and the landscape’s susceptibility to desertification under different climate drivers and management conditions [21, 22].

Deterministic mechanisms of pattern formation have been widely studied [23, 24, 25] with a number of applications to environmental processes [26, 8, 6, 27, 28, 29, 30, 31]. Stochastic models have only been developed more recently [32, 33]. They explain pattern formation as a noise-induced effect in the sense that patterns can emerge as a consequence of the randomness of the system’s fluctuations. These random drivers have often been related [34, 35] to a symmetry-breaking instability. They destabilize a homogeneous (and, thus, symmetric) state of the system and determine a transition to an ordered phase, which exhibits a degree of spatial organization. In the thermodynamics literature these order-forming transitions are usually referred to as non-equilibrium transitions, to stress the fundamental difference in the role of noise with respect to the classical case of equilibrium transitions, which exhibit an increase in disorder as the amplitude of internal fluctuations increases.

Here, we propose an overview of the main stochastic processes related to the presence of Gaussian white noise, focusing on the fundamental mechanisms able to induce spatial coherence. We concentrate on Gaussian white noise because it provides a reasonable assumption for the unavoidable randomness of real systems – the spatial and temporal scales of the Gaussian white noise are much shorter than the characteristic scales over which the spatio-temporal

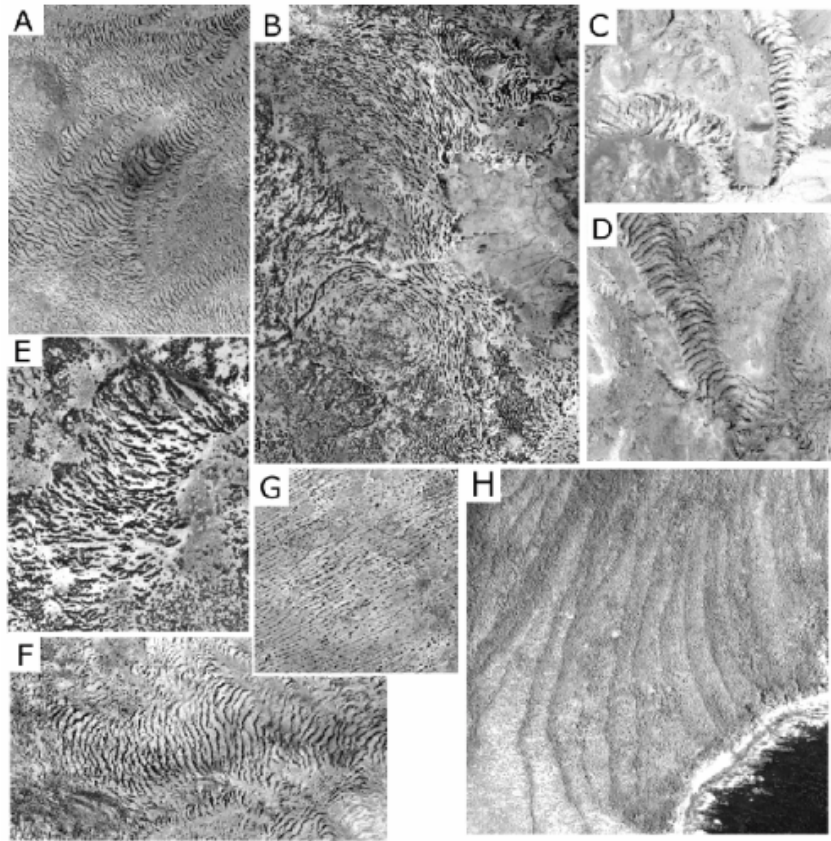


Figure 1: Example of aerial photographs showing vegetation patterns (tiger bush). (a) Somalia ( $9^{\circ}20'N$ ,  $48^{\circ}46'E$ ), (b) Niger ( $13^{\circ}21'N$ ,  $2^{\circ}5'E$ ), (c) Somalia ( $9^{\circ}32'N$ ,  $49^{\circ}19'E$ ), (d) Somalia ( $9^{\circ}43'N$ ,  $49^{\circ}17'E$ ), (e) Niger ( $13^{\circ}24'N$ ,  $1^{\circ}57'E$ ), (f) Somalia ( $7^{\circ}41'N$ ,  $48^{\circ}0'E$ ), (g) Senegal ( $15^{\circ}6'N$ ,  $15^{\circ}16'W$ ), and (h) Argentina ( $54^{\circ}51'S$ ,  $65^{\circ}17'W$ ). Google Earth imagery © Google Inc. Used with permission.

dynamics of the field variable are evolving – and, therefore, it is typically adopted in stochastic modeling. Moreover, the white noise assumption simplifies analytical and numerical calculations. We call “patterned” a field that exhibits an ordered state with organized spatial structures. This general definition, including both periodic as well as multiscale patterns, is often adopted in the environmental sciences, where the number of different processes can prevent the organization of the system with a specific wavelength. We define multiscale those patterns that are *scale-free* [36, 37], in the sense that spatial coherence emerges without showing a clear periodicity. Depending on their behavior in time, patterns can be also classified as steady or transient, on the basis of whether the spatial coherence is constant in time or appears only temporarily with the tendency to fade out with time. Steady patterns are here defined as statistically steady in time. This means that, once the steady state is reached, the field variable can locally assume different values, but the mean characteristics of ordered spatial structures remains the same. In the case of oscillating patterns the spatial coherence instead fluctuates with time and patterns periodically emerge and disappear.

In Section 2 a mathematical model of the spatio-temporal dynamics is introduced. We then consider two simple stochastic models (Sections 3 and 4), in order to clarify the interplay among three fundamental mechanisms: the local dynamics, the noise component and the spatial coupling. Pattern formation with temporal phase transition is described in Section 5. Concluding remarks are given in Section 6. Analytical prognostic tools and numerical algorithms for pattern detection are treated in Appendix A.

## 2. Stochastic Modeling

The spatio-temporal dynamics of the state variable,  $\phi$ , can be expressed, at any point  $\mathbf{r} = (x, y)$ , as the sum of four terms: (i) a function,  $f(\phi)$ , of local dynamics; (ii) a multiplicative noise term,  $g(\phi)\xi(\mathbf{r}, t)$ ; (iii) a term,  $D\mathcal{L}[\phi]$ , accounting for the spatial interactions with the other points of the domain, and (iv) an additive random component  $\xi_a(\mathbf{r}, t)$ . Therefore, the dynamics read

$$\frac{\partial \phi}{\partial t} = f(\phi) + g(\phi)\xi(\mathbf{r}, t) + D\mathcal{L}[\phi] + \xi_a(\mathbf{r}, t), \quad (1)$$

where  $\mathcal{L}$  is an operator expressing the spatial coupling of the dynamics, while  $D$  is the strength of the spatial coupling. The description of the spatio-temporal stochastic resonance and coherence – two mechanisms of noise-induced pattern formation that need the cooperation of a temporal periodicity – is not included in this review. Thus, we will concentrate on the case of dynamics in which the state of the system is determined by one state variable,  $\phi$ , without time-dependent forcing terms.

The crucial point in the dynamical systems here investigated is that pattern formation is noise-induced, i.e., it is due to random fluctuations and does not occur in the deterministic counterpart of the dynamics. In fact, these symmetry-breaking states vanish as the noise intensity drops below a critical value depending on the specific spatiotemporal stochastic model considered. For some configurations these noise-induced transitions are re-entrant. This means that the ordered phase is reached beyond a threshold but is then destroyed if the noise intensity exceeds a higher threshold. In these cases, the noise has a constructive effect only when its intensity is within a certain interval of values. Smaller or larger values are either too weak or too strong to induce ordered structures. We consider a white (in time and space) Gaussian noise with zero mean and correlation given by

$$\langle \xi(\mathbf{r}, t)\xi(\mathbf{r}', t') \rangle = 2s\delta(\mathbf{r} - \mathbf{r}')\delta(t - t'), \quad (2)$$

where  $s$  is the noise intensity. We interpret the Langevin equation (1) in the Stratonovich sense. In this case  $\langle g(\phi)\xi(\phi) \rangle = s\langle g(\phi)g'(\phi) \rangle$ , where  $g'(\phi)$  is the derivative of  $g$  with respect to  $\phi$ . In contrast, under Ito interpretation, one has  $\langle g(\phi)\xi(\phi) \rangle = 0$  [32, 33].

A number of mathematical models can be used to express the spatial coupling in spatiotemporal dynamics. We call *pattern-forming* those operators that, under suitable conditions, are able to generate periodic patterns even without noise. In contrast, non-pattern-forming operators are able to give spatial coherence inducing multiscale patterns, without selecting a clear dominant length scale. A typical example of non-pattern-forming operator is the Laplacian,

$$\mathcal{L}[\phi] = \nabla^2 \phi = \frac{\partial^2 \phi}{\partial x^2} + \frac{\partial^2 \phi}{\partial y^2}, \quad (3)$$

which is widely used to represent the effect of the diffusion mechanisms in a dynamical system. This operator accounts for spatial interactions between a point of the domain and its nearest neighbors, and is therefore considered as a short-range spatial coupling.

A mathematical structure able to describe pattern-forming couplings is instead the Swift-Hohenberg operator

$$SH[\phi] = -(\nabla^2 + k_0^2)^2 \phi, \quad (4)$$

where  $k_0$  is a parameter corresponding to the wavenumber selected by the spatial interactions. It should be noted that, beside the effect of short-range interactions expressed by the Laplacian operator  $\nabla^2$ , the biharmonic term,  $\nabla^4$ , accounts for long-range interactions. Indeed, in a finite difference discrete representation of equation (4) the biharmonic operator accounts for interactions with points of the domain located next to the nearest neighbors. The Swift-Hohenberg operator is one of the simplest types of coupling able to account for both short and long range interactions and to form periodic patterns. For this reason it has been widely adopted in different applications [24, 32]. The structure (4) was first introduced by [1] to study the effect of hydrodynamic fluctuations in systems exhibiting Rayleigh-Bénard convection [25]. However, the interplay between short and long range interactions expressed by (4) is a recurrent mechanism of pattern formation in nature. For example, in landscape ecology, cooperative interactions for vegetation growth – such as mulching, shading, absence of biological crusts [38, 39, 40, 41, 42] – occur in the short range of plants' crown areas, while inhibitory effects hindering vegetation establishment – such as competition for water and nutrients through the root system [31, 38, 43, 44] – typically occur at larger distances.

### 3. Additive noise

Consider the stochastic model

$$\frac{\partial \phi}{\partial t} = a\phi + D\mathcal{L}[\phi] + \xi_a(\mathbf{r}, t) \quad (5)$$

where  $\phi(\mathbf{r}, t)$  is the scalar field,  $a$  is a parameter, and  $\xi_a(\mathbf{r}, t)$  is a zero-mean Gaussian white (in space and time) noise with intensity  $s_a$ . Equation (5) is the prototype model used to show how patterns may occur in the absence of multiplicative noise (i.e.,  $g(\phi) = 0$  in the general equation (1)) and of a time-dependent forcing. We concentrate on linear deterministic dynamics to point out the fundamental mechanisms able to induce pattern formation, without invoking nonlinearities, which in this case do not substantially change the pattern properties. In so doing, we present very simple, though common and realistic, models of pattern formation. In this section we will first study the case where  $\mathcal{L}[\phi]$  is a pattern forming spatial coupling.

#### 3.1. Pattern forming coupling

The prototype model is

$$\frac{\partial \phi}{\partial t} = a\phi - D(\nabla^2 + k_0^2)^2 \phi + \xi_a. \quad (6)$$

The deterministic part of the dynamics does not generate patterns for any value of  $a$ : if  $a < 0$  the system is damped to zero without showing any spatial coherence, if  $a$  is positive, no steady states exist and the dynamics of  $\phi$  diverge without displaying any ordered spatial structures. Additive noise,  $\xi_a$ , is able to keep the dynamics away from the homogenous deterministic steady state even though in the underlying deterministic dynamics  $f(\phi)$  would tend to cause the convergence to the homogenous state. In these conditions patterns emerge and are continuously sustained by noise. These patterns are noise-induced in that they disappear and the homogeneous stable state  $\phi = 0$  is restored if the noise intensity is set to zero. Figure 2 reports some results from numerical simulations, including the spatial field, the probability density function (pdf) of  $\phi$ , and the azimuth-averaged power spectrum and the structure function of the stochastic model (6). More details on the numerical methods are provided in Appendix A. The results confirm that a very clear and statistically stable pattern occurs in spite of  $a$  being negative: the noise component moves the dynamics away from the deterministic steady state  $\phi_0 = 0$  and allows the spatial differential terms to drive the field into a patterned state with wave length  $2\pi/k_0$ .

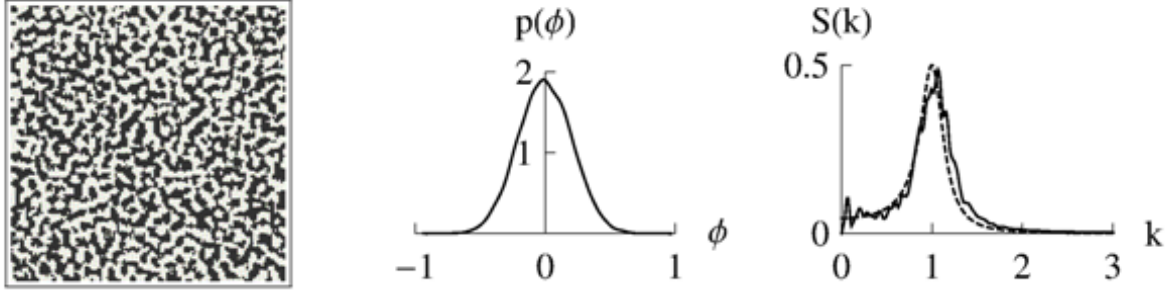


Figure 2: Model (6) at  $t = 100$ , with  $a = -1$ ,  $D = 10$ ,  $k_0 = 1$ , and  $s_a = 0.5$ . First panel: numerical simulations of the field. Black and white tones are used for positive and negative values of  $\phi$ , respectively. Second panel: pdf of  $\phi$ . Third panel: azimuthal-averaged power spectrum (solid: numerical simulations, dotted: structure function).

This pattern-inducing role of the noise can be detected through the structure function, as defined in Appendix A.3. Using Equation (A.12) one obtains

$$S_{st}(\mathbf{k}) = \frac{s_a}{D(-k^2 + k_0^2)^2 - a}. \quad (7)$$

Thus, even for  $a < 0$  the steady state structure function has a maximum at  $k = k_0$  (see third row of figure 2, where the numerical power spectrum and the structure function are compared at steady state). This result confirms that additive random fluctuations are able to induce a stable pattern. When the noise is absent ( $s_a = 0$ ) the steady state structure function is uniformly null and no patterns form.

The normal mode stability analysis (see Appendix A.1) is unable to detect the occurrence of patterns. In fact, according to this analysis no pattern should emerge when  $a < 0$ . Similarly, the generalized mean field technique (see Appendix A.4.1) is unable to capture the constructive role of additive noise.

The classical mean field technique (see Appendix A.4.2) leads to

$$\frac{d\phi_i}{dt} = f(\phi_i) + g(\phi_i)\xi_i - Dk_0^4\phi_i - D\left(\frac{20}{\Delta^4} - \frac{8k_0^2}{\Delta^2}\right)(\phi_i - m) + \xi_{a,i}, \quad (8)$$

where  $\Delta$  is the spatial step (see Appendix A). This analysis shows that the order parameter,  $m$ , does not change, i.e., the periodic patterns induced by additive noise do not entail phase transitions. The pdfs of the field variable,  $\phi$ , shown in Figure 2, confirm the theoretical findings from the mean field analysis. Indeed, one observes that the pdfs remain unimodal and symmetrical at any time, with the mean at  $\phi = 0$  in spite of the appearance of patterns.

### 3.2. Non-pattern forming coupling

In this section, we consider the same interplay between the local deterministic component,  $f(\phi)$ , and the noise component investigated in the previous section. However, we consider a spatial coupling which is not able to select a specific wavelength. The prototype model becomes

$$\frac{\partial\phi}{\partial t} = a\phi + D\nabla^2\phi + \xi_a. \quad (9)$$

The introduction of the additive random component allows one to obtain very interesting patterned fields. The effect of additive noise is even more surprising than with a pattern-forming coupling. In that case, (unsteady) patterns were in fact already potentially present in the deterministic dynamics (see Section 3.1). In contrast, here the deterministic dynamics does not reveal any transient spatial coherence.

Considering the steady state structure function, one obtains

$$S(\mathbf{k}, t) = \frac{s_a}{Dk^2 - a} \quad (10)$$

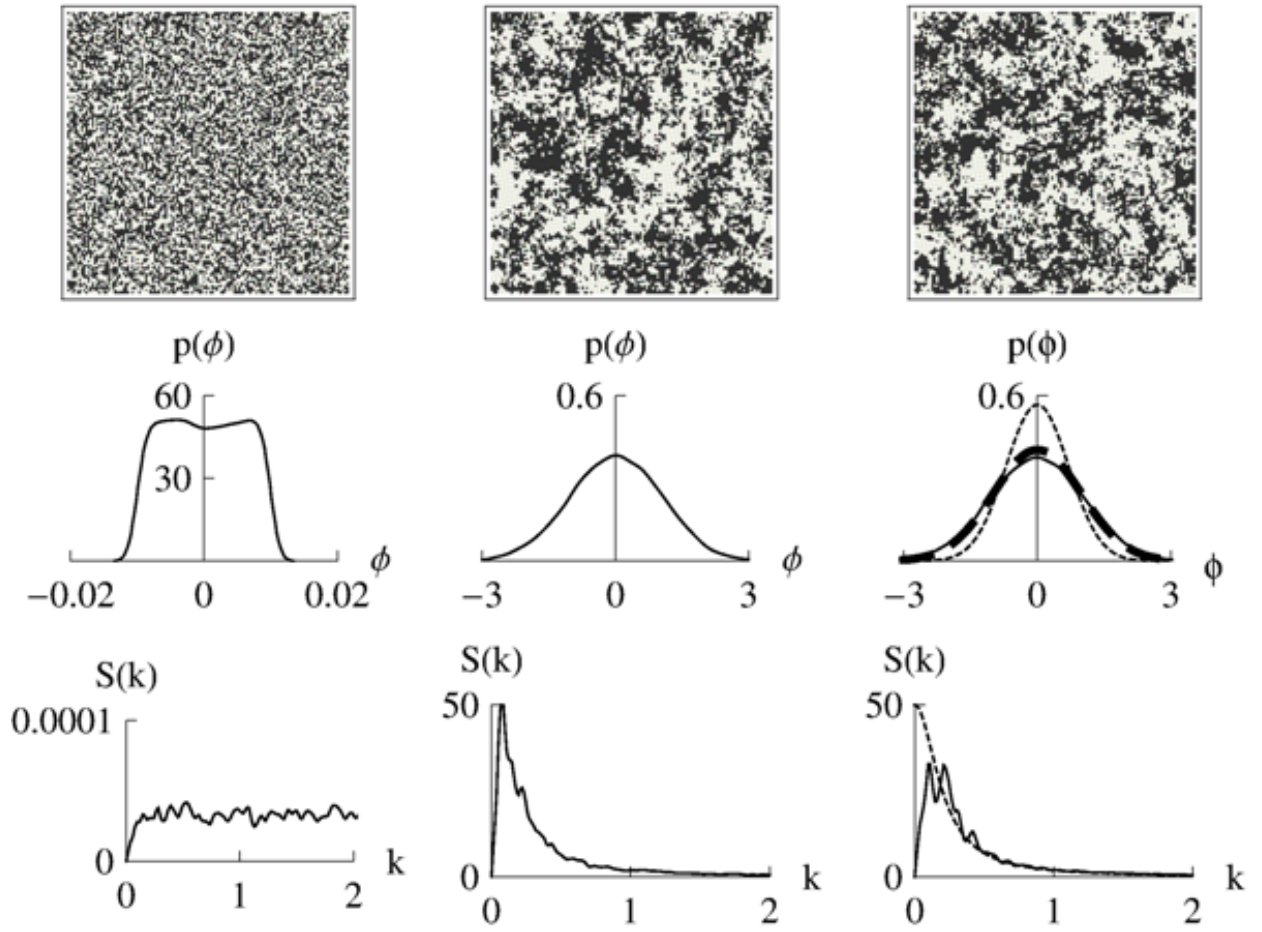


Figure 3: Model (9) with  $\alpha = -0.1$ ,  $D = 2.5$ , and  $s_a = 5$ . The columns refers to 0, 200, and 400 time units. First row: numerical simulations of the field. Second row: pdfs of  $\phi$  (solid: numerical simulation, dotted: classic mean-field, dashed: corrected mean-field). Third row: azimuthal-averaged power spectrum (solid: numerical simulations, dotted: structure function).

which exhibits a maximum at  $k = 0$  (see third row of figure 3, where the numerical power spectrum and the structure function are shown at steady state). No specific periodicity is selected, but a range of wave numbers close to zero compete to give rise to multiscale patterns. However, since it is difficult to predict the characteristics of these patterns only by looking at the properties of the structure function, we have to rely mostly on numerical simulations.

An example is reported in figure 3, where results are shown in terms of the spatial field, the pdf, the azimuth-averaged power spectrum and the structure function. As expected from the analysis of the structure function, no clear periodicity is visible, but many wave lengths are present. The boundaries of the coherence regions are irregular and these spatial structures fall then in the class of multiscale fringed patterns, which are especially relevant in the environmental sciences [36, 37]. In fact, a number of environmental patterns exhibit a spatial behavior very similar to the one shown in figure 3. A typical example is the distribution of vegetated sites in semi-arid environments [8].

In this case, other prognostic tools, such as the modal stability analysis and the generalized mean field theory, fail to provide useful indications. The pdf is unimodal (see the second row of the figure 3) and its mean coincides with the basic homogeneous stable state (i.e.,  $m = \phi_0 = 0$ ). Therefore, there is no phase transition. This behavior follows the general rule that Gaussian additive noise is unable to give rise to phase transitions (i.e. changes of  $m$ ) for any type of spatial coupling.

Pattern formation induced by additive noise is usually introduced in the scientific literature as a remarkable example of noisy precursor near a deterministic pattern-forming bifurcation [32]. The additive noise acts on a deterministic system that exhibits a bifurcation point between a homogeneous stable state and a stable patterned state (an example is the Ginzburg-Landau model [33, 32]). In this case, the role of the additive noise is to unveil the intrinsic spatial periodicity of the deterministic system even before reaching the pattern-forming bifurcation.

This point of view suggests that a deterministic bifurcation is necessary in order to have an additive noise generating a pattern. The example with  $f(\phi) = a\phi$  we have just presented demonstrates, instead, that this is not necessarily true. In this case there is no bifurcation since the dynamical system diverges when  $a > 0$ . Therefore, the existence of a deterministic bifurcation is not a necessary condition for pattern formation. Patterns emerge as an effect of additive noise, which unveils the capability of the deterministic component of the dynamical system to induce transient periodic patterns also when the asymptotic stable state is homogenous. Thus, noise exploits this capability and hampers patterns to disappear.

Moreover, it should be noted that the presence of nonlinear components in the deterministic dynamics does not substantially change any of the previous results. The fine details of the patterns can change, but neither their stable occurrence nor their dominant wave length (if detectable) changes.

#### 4. Multiplicative noise

The cooperation between multiplicative noise and spatial coupling is based on two key actions: (i) the multiplicative random component temporarily destabilizes the homogeneous stable state,  $\phi_0$ , of the underlying deterministic dynamics, and (ii) the spatial coupling acts during this instability, thereby generating and stabilizing a pattern. The basic model is

$$\frac{\partial \phi}{\partial t} = f(\phi) + g(\phi)\xi(\mathbf{r}, t) + D\mathcal{L}[\phi], \quad (11)$$

where, with respect to the general equation (1),  $\xi_a$  has been eliminated in order to isolate the role of the multiplicative noise.  $\xi$  is a zero-average Gaussian white noise with intensity  $s$ . We indicate with  $\phi_0$  the stable homogeneous state of the system in the deterministic case. Namely,  $\phi(\mathbf{r}, t) = \phi_0$  is a homogeneous solution of (11) when  $s = 0$  (i.e.,  $f(\phi_0) = 0$  because  $\mathcal{L}[\phi] = 0$  in homogeneous states). Moreover, we consider cases where  $g(\phi_0) = 0$ , so that the noise does not have the possibility to destabilize the homogeneous steady state.

The analytical tools detecting the possible presence of the short term instability are described in Appendix A.2. For values of  $s$  lower than a critical value,  $s < s_c$ , the state variable  $\phi(\mathbf{x}, t)$  experiences fluctuations about  $\phi_0$  but noise does not play any constructive role. The system remains blocked in the disordered phase and no patterns occur. Only transiently, the spatial coupling might be able to induce patterns that disappear as the system approaches its steady state. Conversely, when the noise increases above a critical level,  $s > s_c$ , the spatial term can take advantage of the noise-induced short term instability and prevent that the displacement from the homogeneous equilibrium state decays to zero. In this way, the spatial coupling traps the system in a new ordered state, maintaining the dynamics far from

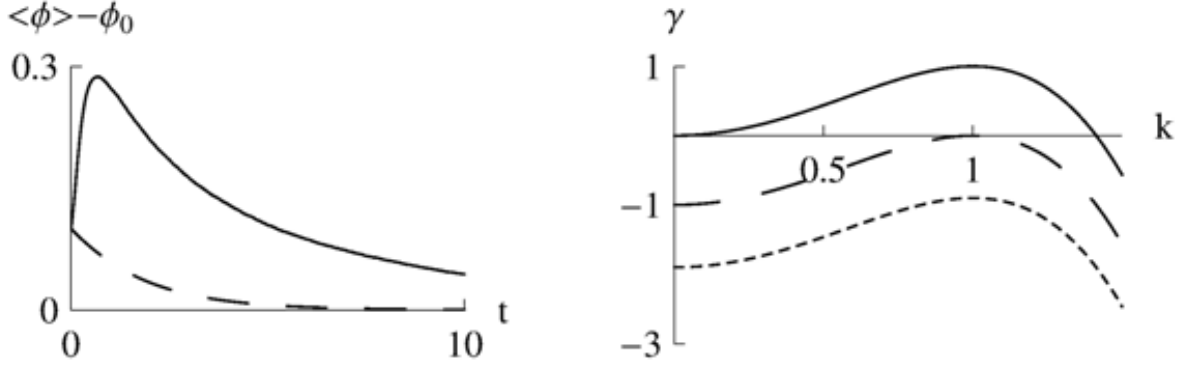


Figure 4: (a) Behavior of  $\langle \phi \rangle - \phi_0$  obtained as ensemble average of  $10^6$  realizations of the model (13) with  $a = -1$ . The initial condition is  $\phi = 0.1$ ,  $s = 0.5$  and  $s = 5$  for the dashed and solid curves, respectively. (b) Dispersion relation of the model (12), with  $s = 0.1, 1, 2$  (dotted, dashed and solid curves, respectively),  $a = -1$ ,  $D = 1$ , and  $k_0 = 1$ .

the state  $\phi_0$ . Equation (11) is here interpreted in the Stratonovich sense, where  $\langle g(\phi)\xi(\phi) \rangle = s\langle g(\phi)g'(\phi) \rangle$ , while under Ito's interpretation no short-term instability occurs, as  $\langle g(\phi)\xi(\phi) \rangle = 0$  (see Appendix A.2).

Other works have been proposed to describe the role of multiplicative noise in pattern formation and phase transitions [34, 35, 45], and to show how multiplicative noise can induce periodic patterns [46, 33]. However, they all present quite complicate non linear expressions to represent the local dynamics and the noise terms, so that their physical interpretation is not always straightforward. For example, when  $g(\phi_0) \neq 0$ , the noise plays a role similar to  $\xi_a(\mathbf{r}, t)$  in Eq. (5). Moreover, the results of those models are qualitatively similar to those described in the following sections, provided that the interplay between short-term instability and spatial coupling remains the same.

#### 4.1. Pattern forming coupling

To illustrate how pattern formation can be driven by multiplicative noise in the presence of a pattern-forming spacial coupling, we consider the model

$$\frac{\partial \phi}{\partial t} = a\phi - \phi^3 + \phi\xi - D(k_0^2 + \nabla^2)^2\phi, \quad (12)$$

where  $a$  is a negative number, the random component is modulated by a function  $g(\phi) = \phi$ , and  $\xi$  is a zero mean white Gaussian noise, with intensity  $s$ . The local dynamics are  $f(\phi) = a\phi - \phi^3$ , where the nonlinear term  $-\phi^3$  has been introduced to avoid that the dynamics diverge. Indeed, the linear term prevents the dynamics from relaxing to a homogeneous steady state, thereby allowing the spatial terms to be different from zero, while the nonlinear term prevents the divergence of the dynamics (i.e., it ensures the convergence to a statistically stable state). The deterministic homogeneous stable state, obtained as a solution of  $f(\phi_0) = 0$ , is  $\phi(\mathbf{r}, t) = \phi_0 = 0$ . From the short-term instability (see Appendix A.2) one has that  $\phi_0$  is stable for  $s < -a$  and becomes unstable for  $s > -a$ . To show this point, Figure 4a reports the time behavior of the ensemble average of a number of numerically evaluated realizations of the zero-dimensional stochastic model obtained eliminating the spatial component from equation (12), that is

$$\frac{d\phi}{dt} = f(\phi) + g(\phi)\xi(t) = a\phi - \phi^3 + \phi\xi(t). \quad (13)$$

It is evident from figure 4a that the growth phase appears only when  $s > s_c = -a$  and at the beginning of simulations (i.e., at short term), while the effect of the initial perturbation disappears in the long run. Mathematically, the short-term instability can be understood by observing that when  $\phi$  is close to zero the disturbance effect due to the (multiplicative) noise tends to prevail on the restoring effect of  $f$ . When  $\phi$  grows, the leading term,  $\phi^3$ , prevails on  $g$  and the local dynamics,  $f$ , tend to restore the state  $\phi_0$ .



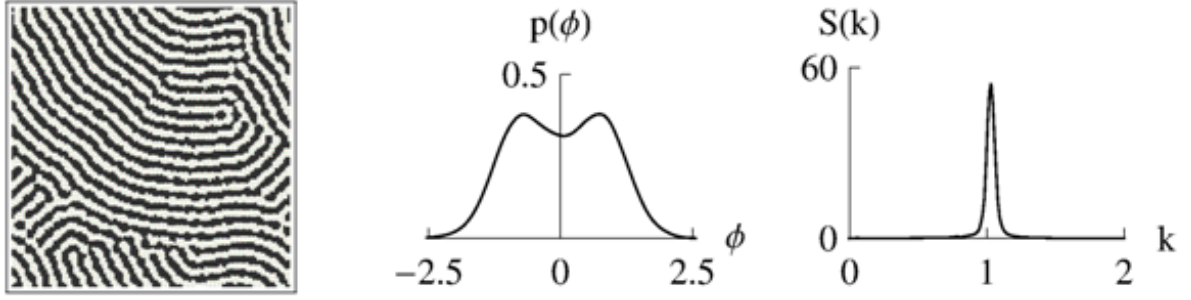


Figure 5: Model (12) at  $t = 100$ , with  $a = -1$ ,  $D = 15$ ,  $k_0 = 1$ ,  $s = 2.5$ . First panel: numerical simulations of the field. Second panel: pdf of  $\phi$ . Third panel: azimuthal-averaged power spectrum.

Once the presence of a short-term instability has been detected, the capability of the spatiotemporal stochastic model (12) to give rise to patterns can be investigated through the stability analysis by normal modes, see Appendix A.1. The dispersion relation is

$$\gamma(k) = a + s - D(k_0^2 - k^2)^2, \quad (14)$$

which provides the same threshold  $s_c$  for the neutral stability found with the short-term instability, while the maximum amplification is for the wavenumber  $k = k_0$  (see figure 4b). It follows that statistically steady periodic patterns, with wave length  $\lambda = 2\pi/k_0$ , emerge when the noise intensity exceeds the threshold  $s_c = -a$ . Moreover, the critical value of the noise intensity for the neutral stability,  $s_c = [-a + D(k_0^2 - k^2)^2]$ , is confirmed by the structure function (see Appendix A.3). The generalized mean-field analysis of the most unstable mode predicts an unconfined region of instability. This means that, if  $s > s_c$ , the system is able to exhibit periodic patterns for any value of  $D$ .

The numerical simulation of the stochastic model (12) confirm these theoretical findings. Figure 5 shows an example of patterns emerging from the simulation. These patterns have the same basic characteristics as those observed in the case of additive noise (see figure 2). They are statistically stable and exhibit a clear dominant wave length corresponding to  $k_0$ . In this case the pdf of the field is weakly bimodal with the zero mean, demonstrating that no phase transition occurs. However, there are some important differences with respect to the case of additive noise. Firstly, the boundaries appear to be more regular when patterns are induced by multiplicative noise. Such aspect is also displayed by the power spectrum of the field, which shows a more sharp peak at  $k_0$  in the case of multiplicative noise (compare the third rows of figures 2 and 5). This difference is due to the fact that multiplicative noise is modulated by the local value of  $\phi$ , and this has the effect to make the boundaries of the pattern more regular because the  $\phi$  field is spatially correlated (from the definition itself of patterned state). Another difference is that patterns induced by additive noise exhibit more stable shapes than those emerging as an effect of multiplicative noise. For example, patterns shown in figure 5 seem to evolve from a labyrinthine shape to a striped shape. Overall, numerical simulations show that patterns induced by additive noise quickly reach their steady state without showing any transient temporal evolution, while those induced by multiplicative noise present a transient behavior, during which they modify their shape until the steady state is reached. The third difference is the possible occurrence of a weak bimodality in the pdf of  $\phi$  in the dynamics driven by multiplicative noise (see figure 5). The presence of such bimodality depends on model structure, parameter values, and field size; however, it generally remains weak.

Let's now look at the effect of nonlinear  $g(\phi)$  terms on the short-term instability. Consider equation (12) with  $a < 0$  and  $g(\phi) = \phi^\alpha$ . If  $\alpha > 1$  no short-term instability occurs. This result is explained interpreting the short-term behavior as a balance between the tendency of  $f(\phi)$  to restore the homogeneous state,  $\phi = \phi_0 = 0$ , and the diverging action of  $g(\phi) \cdot \xi$ . Since  $\phi$  is close to zero, the power  $\alpha > 1$  of the function  $g(\phi)$  reduces the effect of the noise term, which becomes unable to contrast the action of the leading term,  $a\phi$ , of  $f(\phi)$ . Patterns occur only transiently and the field then rapidly decays to the homogeneous state  $\phi_0$ .

Conversely, if  $\alpha < 1$ , short-term instability occurs in that the multiplicative component always overcomes the action of  $f(\phi)$  close to zero. The balance between  $f(\phi)$  and  $g(\phi)\xi$  is reverted when  $\phi$  moves away from  $\phi_0 = 0$ , and this fact

hampers the dynamical system to diverge. In this case, patterns are statistically stable and exhibit the same dominant wave length as those shown in figure 5.

#### 4.2. Non-pattern forming coupling

We explore the capability of spatio-temporal models driven by multiplicative noise to generate patterns when a non-pattern forming spatial coupling is adopted. To focus on the role of the type of spatial operator, we consider the same model as in Section 4.1, but with a diffusive Laplacian operator, namely

$$\frac{\partial \phi}{\partial t} = a\phi - \phi^3 + \phi\xi + D\nabla^2\phi. \quad (15)$$

where  $\xi$  is a zero mean white Gaussian noise, with intensity  $s$ , and equation (15) is interpreted in the Stratonovich sense. The model (15) has a homogeneous deterministic stable state at  $\phi_0 = 0$  and exhibits short-term instability when  $s > s_c = -a$  (see Section 4.1). The dispersion relation obtained with the linear stability analysis reads

$$\gamma(k) = a + s - Dk^2. \quad (16)$$

We can make the following three remarks. First, the value  $s = -a$  of the noise intensity marks the condition of marginal stability. No unstable wave numbers occur when  $s < -a$ , while the wave numbers lower than  $\sqrt{(s + a)/D}$  become unstable if  $s > -a$ . The threshold  $s = -a$  coincides with the one obtained in the short term analysis. Second, the strength,  $D$ , of the spatial diffusive coupling impacts the range of unstable wavenumbers. In particular, the unstable wave numbers decrease when  $D$  increases, consistently with the fact that the diffusive coupling introduces spatial coherence in the random field. However,  $D$  does not impact the occurrence of instability, in that it depends only on the noise intensity. Third, the most (linearly) unstable mode is always  $k_{max} = 0$ , for any  $D$  and provided that  $s > -a$ . The classic mean-field analysis predicts a phase transition for any value of the spatial coupling,  $D$ . In other words, once the critical threshold of noise intensity is exceeded, the system is always able to move to a new ordered state.

Figure 6 shows that the emergence of a pattern with no clear periodicity. It evolves in time and tends to disappear in the long term. The pdf of the field reveals that patterns occur during a phase transition from the initial basic state having order parameter  $m = \phi_0 = 0$  to a new substantially homogeneous state with  $m \neq 0$ . In particular, for the case shown in figure 6 numerical simulations give  $m = 0.8$  for  $t > 100$  time units. Although with diffusive coupling both the cases of additive and multiplicative noise (not shown for sake of brevity) exhibit a well defined peak at  $k = 0$ , numerical simulations show a different scenario (compare figures 6 and 3). While the presence of additive noise produces steady multiscale fringed patterns, multiplicative noise induces only smooth transient patterns. The reason of this different temporal behavior is that, in the multiplicative case, the diffusive operator is unable to maintain the system far from homogeneous condition, in spite of the initial instability. Indeed, to have steady patterns sustained by multiplicative noise the presence of a pattern-forming spatial coupling is necessary. When other types of spatial couplings are considered, they are unable to block the system far from the homogeneous state. In these cases, the spatial coupling interacts with the short-term instability, as detected by the dispersion relation – recall that the stability analysis is performed on an equation that approximates only the first stages of the ensemble average dynamics – but this interaction lasts only until the temporal dynamics are able to sustain the instability. Thereafter, the patterns undergo the same fate as the initial instability, i.e., they tend to disappear. In the long run the main legacy of the spatial coupling is the phase transition (i.e.,  $m \neq 0$ ), though for a homogeneous field. Similarly to the case discussed in Section 4.1, the coherence regions are much smoother than those observed with additive noise. Even in this case, this difference is due to the multiplicative nature of the noise, which entails that the  $g(\phi)\xi$  term is spatially correlated.

### 5. Patterns with temporal phase transition

In this section we consider the extension to spatial systems of noise-induced transitions in purely temporal systems [47]. Such transitions correspond to the occurrence of steady state probability distributions whose modes are different from the equilibrium states of the corresponding deterministic system. A relevant case is represented by systems exhibiting noise-induced bistability. In this case, suitable noise intensities are able to generate pdfs with two modes even though the deterministic dynamics have only one stable state. Two key ingredients are needed to activate this

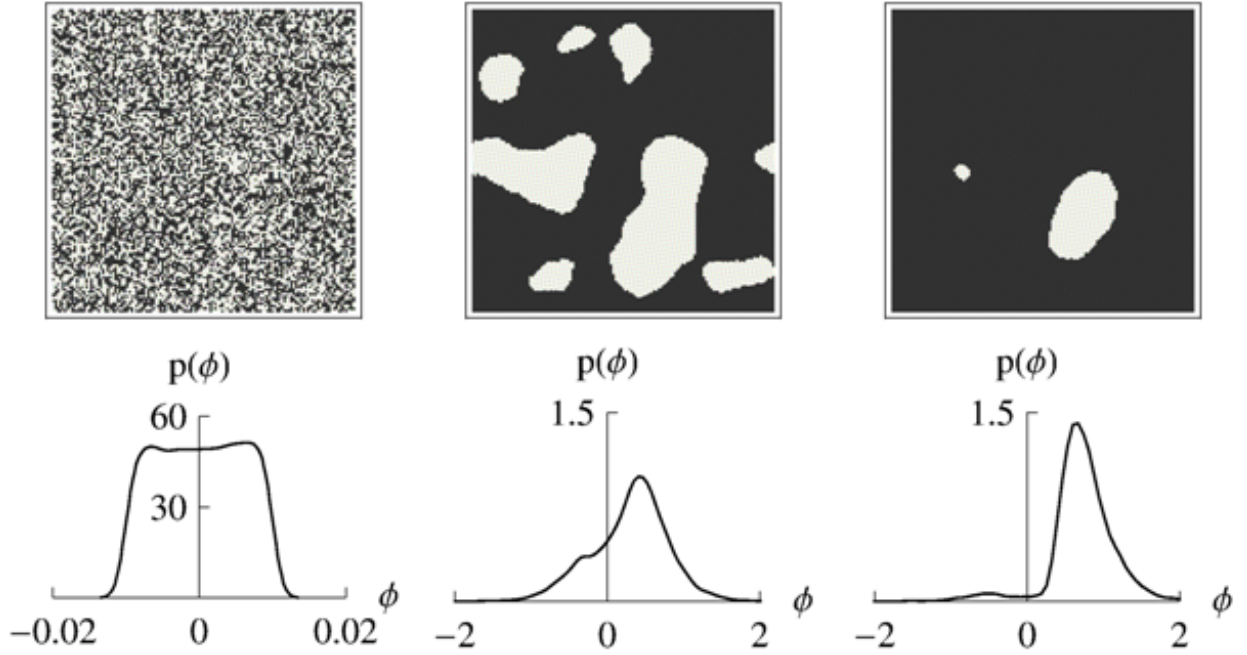


Figure 6: Model (15) with  $a = -1$ ,  $s = 2$ ,  $D = 5$ . The columns refer to 0, 10, and 40 time units. First row: numerical simulations of the field. Second row: pdfs of  $\phi$ .

type of stochastic dynamics. First, a deterministic local kinetics,  $f(\phi)$ , which tends to drive the dynamical system towards the steady state,  $\phi = \phi_0$ . Second, a multiplicative random component that tends to drive the state of the system away from  $\phi = \phi_0$ ; the intensity of this component is generally maximum at  $\phi = \phi_0$ . As a result of the balance between deterministic and stochastic components, bimodal probability distributions of  $\phi$  may emerge at steady state.

In spatiotemporal dynamical systems the spatial coupling could (i) cooperate with the stochastic component to prevent the relaxation imposed by the local dynamics and maintaining the system away from the uniform state,  $\langle \phi \rangle = \phi_0$ , and (ii) give spatial coherence to the field creating a patterned state where the coherent regions correspond to the two modes existing in the underlying temporal dynamics.

The mechanism here discussed is sometimes called *entropy-driven pattern formation* [32] as the dynamical system escapes from the minimum of the potential (i.e.,  $\phi = \phi_0$ ) because of the strength of noise (which is an entropy source). There are two main differences with respect to the case presented in the previous sections: (i) patterns do not result from a short-term instability, and (ii) they emerge even if the noise is interpreted according to Ito's rule.

### 5.1. Model with $g(\phi_0) = 0$

It is interesting to consider what happens when no noise term is present for  $\phi = \phi_0$ , i.e. when  $g(\phi_0) = 0$ . Indeed, in this case the noise component is unable to unlock the system from the deterministic stable state  $\phi_0$  and to sustain the pattern-forming effect of the spatial coupling by maintaining the dynamics away from the homogeneous stable state,  $\phi = \phi_0$ .

We consider the model

$$\frac{\partial \phi}{\partial t} = -a\phi + \phi(1 - \phi)\xi(t) - D(k_0^2 + \nabla^2)^2 \phi, \quad (17)$$

interpreted according to Ito. As in the case of section 3 we concentrate on the case of linear local dynamics to show how patterns may emerge even without invoking nonlinearities in the underlying deterministic dynamics. The purely temporal version of the model (17) (i.e.,  $d\phi/dt = -a\phi + \phi(1 - \phi)\xi$ ) shows a noise-induced transition for  $s_c = 4a$ . The steady state pdf reads

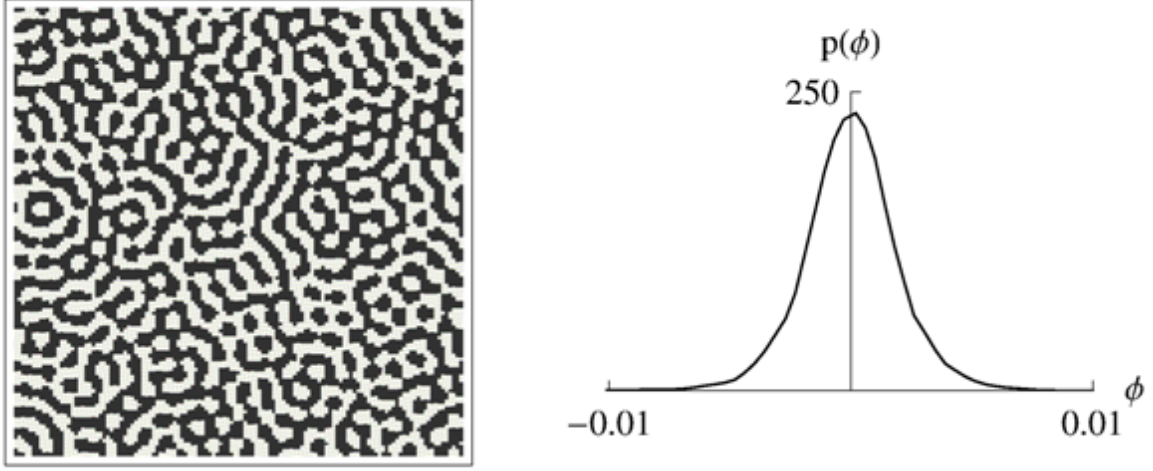


Figure 7: Model (17) under Ito interpretation at  $t = 100$ . The parameters are  $a = 0.001$ ,  $D = 10$ , and  $s = 1$ .

$$p(\phi) = \frac{(1 - \phi)^{\frac{a}{s}-2}}{\phi^{\frac{a}{s}+2}} \text{Exp} \left[ -\frac{a}{s(1 - \phi)} \right] \quad \phi \in ]0, 1[ \quad (18)$$

and has always a mode for  $\phi \rightarrow 0$ , while a second mode occurs when  $s > s_c$ . The onset of bimodality in the model (17) is due to cooperation between the noise and the natural boundaries at  $\phi = 0$  and  $\phi = 1$ . When the noise is sufficiently strong, the system tends to move away from  $\phi = 0$ , but the boundary at  $\phi = 1$  prevents the system from visiting the whole real axis, and an accumulation of probability close to the upper limit of the domain emerges.

Since the noise is interpreted according to Ito, model (17) does not present any noise-induced short term instability (i.e.,  $\langle g(\phi)\xi \rangle = 0$ ). However, the spatial coupling is able to exploit the temporal noise-induced transition and to show patterns. In figure 7 an example is reported. In spite of the pdf of the temporal system displaying a strong bimodality for high enough noise strength, the pdf of the field is unimodal and centered in zero. The generalized mean-field analysis is not able to provide further information.

Patterns can emerge also when in equation (17) the diffusive spatial coupling is used in place of the Swift-Hohenberg operator,

$$\frac{\partial \phi}{\partial t} = -a\phi + \phi(1 - \phi)\xi(t) + D\nabla^2 \phi. \quad (19)$$

Figure 8 shows an example of these patterns. For high enough values of the ratio  $D/a$ , the pdf is unimodal and converges to  $\phi = 1$ . However, the classic mean-field analysis is not able to capture any phase transition of the system.

## 6. Conclusions

We presented different stochastic mechanisms of spatial pattern formation. They all describe spatial coherence and organization as noise-induced phenomena, in the sense that these patterns emerge as an effect of the randomness of the systems drivers.

Additive noise plays a fundamental role when the deterministic local dynamics tends to drive the field variable towards a uniform steady state, while noise is able to maintain the dynamics away from the uniform steady state. The interaction of additive noise with the spatial coupling provides a simple and realistic, mechanism of pattern formation. In the presence of a multiplicative component of adequate intensity the spatial coupling exploits the initial instability of the system to generate ordered structures, which in the absence of noise would tend to disappear in the long run.

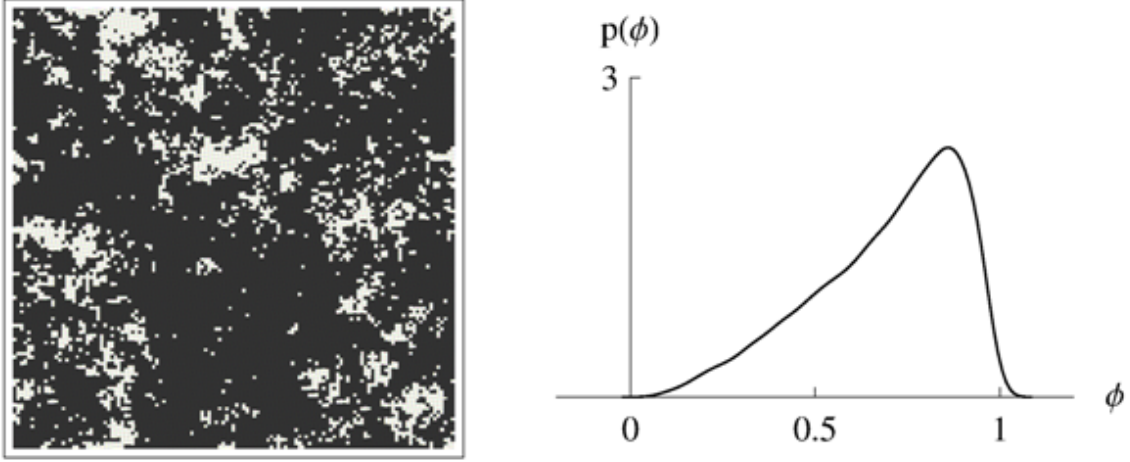


Figure 8: Model (19) at  $t = 300$  under Ito interpretation. The initial conditions are given by uniformly distributed random numbers between  $[0.49, 0.51]$ . Black and white tones are used for the value intervals  $[0.5, 1]$  and  $[0, 0.5]$ , respectively. The parameters are  $a = 0.001$ ,  $D = 25$ ,  $s = 40$ .

The stochastic models presented here show how noise may play a crucial role in pattern formation. However, most of the literature on self-organized morphogenesis in the environment is based on deterministic mechanisms. The limited application of stochastic theories to environmental patterns is likely due to the fact that most of the stochastic models use some specific (and complicated) non linear terms both in the local deterministic dynamics and in the multiplicative function,  $g(\phi)$ , of the noise component. The use of these "ad hoc" functions limits the applicability of these theories to process based environmental modeling. Thus, only few studies have investigated the possible emergence of vegetation patterns as a noise-induced effect. However, because noisy fluctuations – such as those associated with fires, rain, or soil heterogeneity – are a recurrent feature of environmental drivers, their randomness can actually induce spatial coherence in a number of environmental processes, as well as in problems related to front propagation under non-equilibrium conditions [48, 49, 32].

## Appendix A. Analytical and numerical tools

The mathematical complexity of the spatio-temporal models of type (1) hampers general analytical solutions. For this reason, several approximate analytical techniques have been developed in order to obtain some indications of pattern formation. We briefly describe the most important ones.

### Appendix A.1. Linear stability analysis by normal modes

When the occurrence of a dominant wavelength is the main symptom of pattern formation, the first available prognostic tool is provided by the normal mode linear stability analysis. This analysis is based on the idea of disturbing the basic state of the system with a hypothetical infinitesimal perturbation, and to assess whether the perturbation grows in time (in which case patterns have the possibility to emerge) or not. The analysis involves three steps. Firstly, a deterministic equation for the spatiotemporal dynamics of the ensemble average of the field variable,  $\langle \phi \rangle$ , is determined and its homogeneous steady state is found. In general, the multiplicative random component can be expressed as  $\langle g(\phi)\xi \rangle = s\langle g_S(\phi) \rangle$ , where  $g_S(\phi)$  is a function of the state variable. Applying Novikov's theorem [33], for the case of Gaussian white noise interpreted in the Stratonovich sense, we have  $\langle g(\phi)\xi \rangle = s\langle g(\phi)g'(\phi) \rangle$ , i.e.  $g_S(\phi) = g(\phi)g'(\phi)$ . Instead, with Ito's interpretation we have  $\langle g(\phi)\xi \rangle = 0$ . Using equation (1), we find

$$\frac{\partial \langle \phi \rangle}{\partial t} = \langle f(\phi) \rangle + s\langle g_S(\phi) \rangle + D\mathcal{L}[\langle \phi \rangle]. \quad (\text{A.1})$$

The basic state,  $\langle \phi \rangle = \phi_0$ , is obtained as the zero of equation (A.1) at steady state, i.e.  $f(\phi_0) + sg_S(\phi_0) = 0$ .

Equation (A.1) is then linearized, and Taylor's expansion of equation (A.1) around  $\phi = \phi_0$ , truncated to the first order, provides

$$\frac{\partial \langle \phi \rangle}{\partial t} = f'(\phi_0) \langle \phi \rangle + sg'_S(\phi_0) \langle \phi \rangle + D\mathcal{L}[\langle \phi \rangle], \quad (\text{A.2})$$

where  $f'(\phi_0) = \left. \frac{df(\phi)}{d\phi} \right|_{\phi=\phi_0}$  and  $g'_S(\phi_0) = \left. \frac{dg_S(\phi)}{d\phi} \right|_{\phi=\phi_0}$ . The basic state  $\langle \phi \rangle = \phi_0$  is perturbed (third step) by adding an infinitesimal harmonic perturbation

$$\langle \phi \rangle = \phi_0 + \hat{\phi} e^{\gamma t + i\mathbf{k} \cdot \mathbf{r}}, \quad (\text{A.3})$$

with  $\hat{\phi}$  being the perturbation amplitude,  $\gamma$  the growth factor,  $i = \sqrt{-1}$  the imaginary unit,  $\mathbf{k} = (k_x, k_y)$  the wave number vector of the perturbation, and  $\mathbf{r} = (x, y)$  the coordinate vector. If equation (A.3) is inserted in (A.2), one obtains the so-called *dispersion relation*

$$\gamma(k) = f'(\phi_0) + sg'_S(\phi_0) + Dh_{\mathcal{L}}(k), \quad (\text{A.4})$$

where  $h_{\mathcal{L}}(k)$  is a function of the wave number  $k = |\mathbf{k}|$  which depends on the specific form of spatial coupling  $\mathcal{L}$  considered. From equation (A.4) the threshold value of the noise intensity is easily obtained by setting the marginal condition,  $\gamma = 0$

$$s_c = -\frac{f'(\phi_0) + Dh_{\mathcal{L}}(k)}{g'_S(\phi_0)}, \quad (\text{A.5})$$

c When  $s > s_c$ , the growth factor,  $\gamma$ , is positive and spatial patterns may occur.

#### Appendix A.2. Short-term instability

A second tool can be used to assess the possible short term instability in the dynamical system. The transient instability is important because it tends to move the dynamics away from the basic state  $\langle \phi \rangle = \phi_0$ . If this phenomenon is accompanied by a suitable spatial coupling, the system can be trapped in a new ordered state. The first steps of the stability analysis are the same as those described in Appendix A.1, and lead to Eq. (A.1). Since we are here interested in the initial evolution of small displacements from  $\phi_0$ , we can assume  $\langle f(\phi) \rangle \approx f(\langle \phi \rangle)$  and  $\langle g_S(\phi) \rangle \approx g_S(\langle \phi \rangle)$ . For the same reason, we can also neglect the spatial gradients of the fluctuations assuming that in the short term they are small. Equation (A.1) can be approximated at any point of the field as [32]

$$\frac{d\langle \phi \rangle}{dt} \approx f(\langle \phi \rangle) + sg_S(\langle \phi \rangle) = f_{eff}(\langle \phi \rangle), \quad (\text{A.6})$$

where  $f_{eff}$  is often indicated as the effective kinetics. The short term stability analysis of the state  $\phi_0$  by equation (A.6) concerns only the temporal dynamics at a generic point of the field.

Equation (A.6) clearly shows that noise can destabilize the deterministically stable state  $\phi_0$ . This can happen in two possible ways: (i) when the roots of  $f_{eff}(\langle \phi \rangle) = 0$  do not coincide with those of  $f(\langle \phi \rangle) = 0$  or (ii) when the state  $\phi_0$  remains a zero of the r.h.s. of equation (A.6), but sufficiently high noise intensities destabilize this state an unstable one; this occurs when the following condition is met

$$\left. \frac{df_{eff}}{d\langle \phi \rangle} \right|_{\phi_0} \geq 0. \quad (\text{A.7})$$

In both cases noise has to be multiplicative for a transition to occur. The noise threshold  $s_c$  can be obtained by setting the inequality in (A.7) equal to zero. The condition (A.7) derives from the first-order truncated Taylor expansion of the function  $f_{eff}$  around  $\phi_0$ , which yields

$$\frac{d\langle \phi \rangle}{dt} \approx \left. \frac{df_{eff}}{d\langle \phi \rangle} \right|_{\phi_0} \langle \phi \rangle. \quad (\text{A.8})$$

When  $f_{eff}(\phi_0) = 0$ , the sign of the coefficient of  $\langle\phi\rangle$  on the r.h.s. of the previous relation determines the stability of small perturbations around  $\phi_0$ .

When the noise is additive the effective kinetics are  $f_{eff}(\langle\phi\rangle) = f(\langle\phi\rangle)$ . Thus, the stable states of (A.6) are the same as those of the deterministic counterpart of the process.

It is also worth stressing the impact of the type of noise and of its interpretation. While in the Stratonovich case,  $g_S(\phi) = sg(\phi)g'(\phi)$ , using Ito interpretation we have  $g_S(\phi) = 0$ . Therefore, the noise-induced instability is possible only in the Stratonovich interpretation of the Langevin equation (1) and it cannot occur when Ito's framework is adopted.

### Appendix A.3. Structure function

The presence of patterns modifies the correlation structure of the field. Instead of considering the correlation function, this method analyzes its Fourier transform in space, which is known with the name of structure function and defined as  $S(\mathbf{k}, t) = \langle \hat{\phi}(\mathbf{k}, t) \hat{\phi}(-\mathbf{k}, t) \rangle$ , where  $\hat{\phi}(-\mathbf{k}, t)$  is the Fourier transform of  $\phi(\mathbf{r}, t)$  and  $\mathbf{k} = (k_x, k_y)$  is the wave number vector. The structure function is therefore equal to the power spectrum of the field  $\phi$ . The first-order temporal derivative of the structure function reads

$$\frac{\partial S(\mathbf{k}, t)}{\partial t} = \left\langle \frac{\partial \hat{\phi}(\mathbf{k}, t)}{\partial t} \hat{\phi}(-\mathbf{k}, t) \right\rangle + \left\langle \frac{\partial \hat{\phi}(-\mathbf{k}, t)}{\partial t} \hat{\phi}(\mathbf{k}, t) \right\rangle. \quad (\text{A.9})$$

By taking the Fourier transform of the linearized version of Eq. (1) (with  $F(t) = 0$ ), which is obtained by following similar steps to those leading to equation (A.2), and considering the noise terms as white in space, we obtain

$$\frac{\partial \hat{\phi}(\mathbf{k}, t)}{\partial t} = f'(\phi_0) \hat{\phi}(\mathbf{k}, t) + g'(\phi_0) \hat{\phi}(\mathbf{k}, t) \xi(t) + \xi_a(t) + Dh_{\mathcal{L}}(k) \hat{\phi}(\mathbf{k}, t), \quad (\text{A.10})$$

where  $h_{\mathcal{L}}(k)$  is the same operator already defined in Appendix A.1. By substituting Eq. (A.10) into Eq. (A.9) and using Novikov's theorem [33] to express the terms  $\langle \hat{\phi}(\mathbf{k}, t) \hat{\phi}(-\mathbf{k}, t) \xi(t) \rangle = sS(\mathbf{k}, t)$  and  $\langle \hat{\phi}(\pm\mathbf{k}, t) \xi_a(t) \rangle = s_a$  (where  $s_a$  is the intensity of the additive white Gaussian noise), we obtain

$$\frac{\partial S(\mathbf{k}, t)}{\partial t} = 2[f'(\phi_0) + Dh_{\mathcal{L}}(k) + g'(\phi_0)s]S(\mathbf{k}, t) + 2s_a \quad (\text{A.11})$$

At steady state the structure function reads

$$S_{st}(\mathbf{k}) = -\frac{s_a}{[f'(\phi_0) + Dh_{\mathcal{L}}(k) + g'(\phi_0)s]}. \quad (\text{A.12})$$

Eq. (A.12) can be investigated to understand if periodic patterns, corresponding to a maximum of the structure function for wave numbers  $k$  different from zero, are expected to appear. Equation (A.12) shows that the additive noise is fundamental to have a non-null steady-state structure function.

### Appendix A.4. Mean-field analysis

The mean-field theory is typically used to provide an approximated solution of stochastic partial differential equations for spatially-extended systems. The method is valuable mainly for a qualitative analysis of (stochastic) spatiotemporal dynamics [34, 35, 50, 51].

The mean field technique adopts a finite difference representation of the stochastic spatiotemporal dynamics (1)

$$\frac{d\phi_i}{dt} = f(\phi_i) + g(\phi_i) \cdot \xi_i(t) + D \cdot l(\phi_i, \phi_j) + h(\phi_i) \cdot F(t) + \xi_{a,i}(t), \quad (\text{A.13})$$

where  $\phi_i$ ,  $\xi_i$ , and  $\xi_{a,i}$  are the values of  $\phi$ ,  $\xi$ , and  $\xi_a$  at site  $i$ , respectively,  $i$  runs across all the cells of the discretized domain, and  $j \in nm(i)$  refers to the neighbors of the  $i$ -th site involved in the discretized representation,  $l(\phi_i, \phi_j)$ , of the specific spatial coupling considered. A general expression for  $l(\phi_i, \phi_j)$  is

$$l(\phi_i, \phi_j) = w_i \phi_i + \sum_{j \in nm(i)} w_j \phi_j, \quad (\text{A.14})$$



where the number of neighbors,  $nn(i)$ , and the weighting factors  $w_i$  and  $w_j$  depend on the specific finite difference scheme adopted to numerically approximate the spatial operator [52]. The analytical solution of equation (A.13) is hampered by the fact that the dynamics of  $\phi_i$  are coupled to that of the neighboring points. To circumvent this issue, the mean field approach assumes that (i) the variables  $\phi_j$  can be approximated by their local ensemble mean,  $\langle\phi_j\rangle$ , and (ii) there is a relation linking  $\langle\phi_j\rangle$  to the ensemble average,  $\langle\phi\rangle$ .

#### Appendix A.4.1. Generalized mean-field theory

To study the stability of the homogeneous steady state with respect to periodic patterns, the pattern is approximated by a harmonic function,

$$\langle\phi_j\rangle = \langle\phi\rangle \cos[\mathbf{k} \cdot (\mathbf{r}_i - \mathbf{r}_j)], \quad (\text{A.15})$$

where  $\mathbf{k} = (k_x, k_y)$  is the wave number vector. The function  $l(\phi_i, \phi_j)$  in equation (A.13) is approximated as

$$l(\phi_i, \phi_j) \approx l_h(\phi_i, \langle\phi\rangle, k_x, k_y) \quad (\text{A.16})$$

where  $l_h(\cdot)$  depends on the spatial coupling considered.

Under the assumption (A.16), the dynamics (A.13) of  $\phi_i$  become independent of those of the neighboring points. Thus, it is possible to determine exact expressions for the steady-state probability distributions  $p_{st}(\phi; \langle\phi\rangle, k_x, k_y)$  of  $\phi$ . The self-consistency condition

$$\langle\phi\rangle = \int_{-\infty}^{+\infty} \phi p_{st}(\phi; \langle\phi\rangle, k_x, k_y) d\phi = F(\langle\phi\rangle, k_x, k_y) \quad (\text{A.17})$$

can be used to obtain the unknown  $\langle\phi\rangle$  as a function of  $k_x$  and  $k_y$ .

The occurrence of solutions of equation (A.17) different from  $\langle\phi\rangle = \phi_0$  (where  $\phi_0$  is the uniform steady state of the system) corresponds to the loss of stability of the uniform steady state with respect to periodic perturbations. It is expected that this loss of stability takes place only for some specific value of the wave numbers  $k_x$  and  $k_y$ .

Other noise-induced phenomena can be investigated with this method. Indeed, spatial pattern formation is not the only interesting noise-induced effect. In fact, modifications of other statistical descriptors of the field can be relevant, too. Modifications of order parameters are known as *phase transitions*. In particular, when the spatio-temporal average,  $m$ , of the state variable at steady state is different from the homogeneous steady state value, a phase transition occurs. Non-equilibrium phase transitions are induced by the random forcing. The occurrence of non-equilibrium phase transition is neither a necessary nor a sufficient condition for noise-induced pattern formation. Non-equilibrium phase transitions imply that noise is able to change the value of the order parameter, but not that ordered geometrical structures necessarily emerge. Conversely, we have shown that noise-induced patterns may emerge even when  $m$  remains unchanged with respect to the disordered case (i.e., no phase transition occur).

#### Appendix A.4.2. Classic mean-field theory

The classic mean field theory can be presented as a simplified version of the generalized mean field. More specifically, it is assumed that all cells have the same mean, which coincides with the spatiotemporal mean of the field. Namely,  $\mathbf{k} = 0$  in equation (A.15), i.e.  $\langle\phi_j\rangle = \langle\phi\rangle = m$ . In this case, equation (A.17) becomes

$$\langle\phi\rangle = \int_{-\infty}^{+\infty} \phi p_{st}(\phi; \langle\phi\rangle) d\phi = F(\langle\phi\rangle). \quad (\text{A.18})$$

The change in the number of solutions of equation (A.18) indicates the existence of a phase transition. The focus of this analysis is not on the appearance of periodic patterns but only on the occurrence of phase transitions. The effectiveness of this standard mean field approximation can be improved by expressing the values of  $\phi_j$  in the neighborhood of point  $i$  as the average between the spatiotemporal mean and the local value of  $\phi$  at point  $i$ , namely  $\phi_j \approx 1/2(\langle\phi\rangle + \phi_i)$ . This correction of the mean field approximation accounts for the dependence of  $\phi_j$  on the local conditions [32].

The analytical tools here described provide in general some insights into pattern formation, but the definitive way to study the noise-induced pattern formation is to numerically simulate the dynamics and assess the emergence of spatial coherence through a comparison with homogeneous or disordered states of the system. In fact, the linear



stability analysis by normal modes and the short-term instability analysis tend to fail when the noise is additive (i.e.  $g = 0$  in Eq. (1)). In this case, both analyses predict stable configurations for any noise intensity and any strength of the spatial coupling. On the other hand, when only multiplicative noise is present (i.e.  $\xi_a = 0$  in Eq. (1)), the structure function does not provide any information on pattern formation, as  $\phi$  tends to remain equal to zero.

The typical numerical approach is to discretize the continuous spatial domain using a regular Cartesian lattice with spacing  $\Delta x = \Delta y = \Delta$ . Here we consider a two-dimensional square lattice with  $128 \times 128$  sites and  $\Delta = 1$ . The original stochastic partial differential equation (1) is then transformed into a system of coupled stochastic ordinary differential equations as in Eq. (A.13). Infinitely vast random fields are generally approximated numerically in a satisfactory way by periodic boundary conditions, which have been used also in this study. Moreover, unless it was otherwise specified, the initial conditions used in the simulations were uniformly distributed random numbers between  $[-0.01, 0.01]$ . Numerical simulations were carried out with the Heun's predictor-corrector scheme [35],[32]. The pdf is obtained from the spatial distribution of  $\phi$  at fixed time and is numerically evaluated at 100 equally spaced intervals,  $\Delta\phi$ , that cover the range of  $\phi$  values.

## References

- [1] J. Swift, P. C. Hohenberg, Hydrodynamics fluctuations at the convective instability, *Phys. Rev. A* **15**, 319 (1977).
- [2] M. M. Wu, G. Ahlers, D. S. Cannell, Thermally-induced fluctuations below the onset of Rayleigh-Bénard convection, *Phys. Rev. Lett.* **75**, 1743 (1995).
- [3] J. W. Shuai, P. Jung, Optimal intracellular calcium signaling, *Phys. Rev. Lett.* **88** (2002).
- [4] B. J. Gluckman, T. I. Netoff, E. J. Neel, W. L. Ditto, M. L. Spano, S. J. Schiff, Stochastic resonance in a neuronal network from mammalian brain, *Phys. Rev. Lett.* **77**, 4098 (1996).
- [5] W. A. Macfadyen, Soil and vegetation in British Somaliland, *Nature* **165**, 121 (1950).
- [6] R. Lefever, O. Lejeune, On the origin of tiger bush, *Bull. Math. Biol.* **59**, 263 (1997).
- [7] C. A. Klausmeier, Regular and irregular patterns in semiarid vegetation, *Science* **284**, 1826 (1999).
- [8] F. Borgogno, P. D'Odorico, F. Laio, L. Ridolfi, Mathematical models of vegetation pattern formation in ecohydrology, *Rev. Geophys.* **47**, RG1005 (2009).
- [9] I. Rodriguez-Iturbe, A. Rinaldo, *Fractal River Basins: Chance and Self-Organization*. Cambridge Univ. Press, Cambridge, U. K. (2001).
- [10] S. Ikeda, G. Parker, *River Meandering*. Water Resources Monograph 12, American Geophysical Union, Washington, DC (1989).
- [11] J. R. L. Allen, *Principles of physical sedimentology*. Cambridge Univ. Press, Cambridge, U. K. (1985).
- [12] A. Ashton, A. B. Murray, O. Arnoult, Formation of coastline features by large-scale instabilities induced by high-angle waves, *Nature* **414**, 296 (2001).
- [13] E. Bird, *Coastal Geomorphology, An Introduction*. Chichester: John Wiley and Sons (2000).
- [14] N. Lancaster, *Geomorphology of desert dunes*. London, New York: Routledge (1995).
- [15] L. P. White, Vegetation stripes on sheet wash surfaces, *J. Ecol.* **59**, 615 (1971).
- [16] C. Montana, The colonization of bare areas in 2-phase mosaics of an arid ecosystem, *J. Ecol.* **80**, 315 (1992).
- [17] J. Eddy, G. S. Humphreys, D. M. Hart, P. B. Mitchell, P. C. Fanning, Vegetation arcs and litter dams: similarities and differences, *Catena* **37**, 57 (1999).
- [18] G. Bergkamp, A. Cerda, A. C. Imeson, Magnitude-frequency analysis of water redistribution along a climate gradient in Spain, *Catena* **37**, 129 (1999).
- [19] N. Barbier, P. Couteron, J. Lejoly, V. Deblauwe, O. Lejeune, Spatial decoupling of facilitation and competition at the origin of gapped vegetation patterns, *J. Ecol.* **94**, 537 (2007).
- [20] L. Ridolfi, P. D'Odorico, F. Laio, Vegetation dynamics induced by phreatophyte-water table interactions, *J. Theor. Biol.* **248**, 301 (2007).
- [21] J. von Hardenberg, E. Meron, M. Shachak, Y. Zarmi, Diversity of vegetation patterns and desertification, *Phys. Rev. Lett.* **87**, 198101 (2001).
- [22] P. D'Odorico, F. Laio, L. Ridolfi, Noise-induced stability in dryland plant ecosystems, *Proc. Natnl. Acad. Sci. USA* **102**, 10819 (2005).
- [23] A. M. Turing, The chemical basis of morphogenesis, *Philos. Trans. R. Soc. London, Ser. B.* **237**, 37 (1952).
- [24] M. C. Cross, P. C. Hohenberg, Pattern-formation outside of equilibrium, *Rev. Mod. Phys.* **65**, 851 (1993).
- [25] S. Chandrasekhar, *Hydrodynamic and Hydromagnetic Stability*. Clarendon, Oxford, U.K. (1961).
- [26] J. D. Murray, *Mathematical Biology*. Springer, Berlin (2002).
- [27] A. Manor, N. M. Shnerb, Origin of Pareto-like spatial distributions in ecosystems, *Phys. Rev. Lett.* **101**, 268104 (2008).
- [28] P. Couteron, O. Lejeune, Periodic spotted patterns in semi-arid vegetation explained by a propagation-inhibition model, *J. Ecol.* **89**, 616 (2001).
- [29] M. Rietkerk, J. Van de Koppel, Regular pattern formation in real ecosystems, *Trends Ecol. Evol.* **23**, 169 (2008).
- [30] S. Kefi, M. Rietkerk, C. L. Alados, Y. Pueyo, V. P. Papanastasis, A. ElAich, P. C. de Ruiter, Spatial vegetation patterns and imminent desertification in Mediterranean arid ecosystems, *Nature* **449**, 213 (2007).
- [31] R. Lefever, N. Barbier, P. Couteron, O. Lejeune, Deeply gapped vegetation patterns: On crown/root allometry, criticality and desertification, *J. Theor. Biol.* **261**, 194 (2009).
- [32] F. Sagues, J. M. Sancho, J. García-Ojalvo, Spatio-temporal order out of noise, *Rev. Mod. Phys.* **79**, 829 (2007).
- [33] J. García-Ojalvo, J. M. Sancho, *Noise in Spatially Extended Systems*. Springer-Verlag New York (1999).
- [34] C. Van den Broeck, J. M. R. Parrondo, R. Toral, Noise-induced nonequilibrium phase transition, *Phys. Rev. Lett.* **73**, 3395 (1994).

- [35] C. van den Broeck, J. M. R. Parrondo, R. Toral, R. Kawai, Nonequilibrium phase transitions induced by multiplicative noise, *Phys. Rev. E* **55**, 4084 (1997).
- [36] A. Manor, N. M. Shnerb, Facilitation, competition, and vegetation patchiness: From scale free distribution to patterns, *J. Theor. Biol.* **253**, 838 (2008).
- [37] J. von Hardenberg, A. Y. Kletter, H. Yizhaq, J. Nathan, E. Meron, Periodic versus scale-free patterns in dryland vegetation. *Proc. R. Soc. B* **277** 1771-1776 (2010).
- [38] O. Lejeune, M. Tlidi, R. Lefever, Vegetation spots and stripes: Dissipative structures in arid landscapes, *Int. J. Quantum Chem.* **98**, 261 (2004).
- [39] P. D'Odorico, K. Caylor, G. S. Okin, T. M. Scanlon, On soil moisture-vegetation feedbacks and their possible effects on the dynamics of dryland ecosystems, *J. Geophys. Res.* **112** (2007).
- [40] X. D. Zeng, S. S. P. Shen, X. B. Zeng, R. E. Dickinson, Multiple equilibrium states and the abrupt transitions in a dynamical system of soil water interacting with vegetation, *Geophys. Res. Lett.* **31** (2004).
- [41] F. Borgogno, P. D'Odorico, F. Laio, L. Ridolfi, Effect of rainfall interannual variability on the stability and resilience of dryland plant ecosystems, *Water Resour. Res.* **43** (2007).
- [42] R. Joffre, S. Rambal, How tree cover influences the water-balance of Mediterranean rangelands, *Ecology* **74**, 570 (1993).
- [43] N. Barbier, P. Couteron, J. Lejoly, V. Deblauwe, O. Lejeune, Self-organized vegetation patterning as a fingerprint of climate and human impact on semi-arid ecosystems, *J. Ecol.* **94**, 537 (2006).
- [44] M. Rietkerk, S. C. Dekker, P. C. de Ruiter, J. van de Koppel, Self-organized patchiness and catastrophic shifts in ecosystems, *Science* **305**, 1926 (2004).
- [45] A. Becker, L. Kramer, Linear Stability Analysis for Bifurcations in Spatially Extended Systems with Fluctuating Control Parameter, *Phys. Rev. Lett.* **73**, 7 (1994).
- [46] J. M. R. Parrondo, C. van den Broeck, J. Buceta, F. J. DeLaRubia, Noise-induced spatial patterns, *Physica A* **224**, 153 (1996).
- [47] W. Horsthemke, R. Lefever, *Noise Induced Transitions. Theory and Applications in Physics, Chemistry, and Biology.* Springer, Berlin (1984).
- [48] J. Armero, J. M. Sancho, J. Casademunt, A. M. Lacasta, L. Ramirez Piscina, F. Sagues, External fluctuations in front propagation, *Phys. Rev. Lett.* **76**, 3045 (1996).
- [49] D. Panja, Effects of fluctuations on propagating fronts, *Phys. Rep.* **393**, 87 (2004).
- [50] J. Buceta, K. Lindenberg, Spatial patterns induced by purely dichotomous disorder, *Phys. Rev. E* **68**, 011103 (2003).
- [51] A. Porporato, P. D'Odorico, Phase Transitions Driven by State-Dependent Poisson Noise, *Phys. Rev. Lett.* **92**, 110601 (2004).
- [52] J. C. Strikwerda, *Finite difference schemes and partial differential equations.* SIAM, Philadelphia (2004).